Hindawi
Advances in Civil Engineering
Volume 2020, Article ID 8840200, 14 pages
https://doi.org/10.1155/2020/8840200

Research Article

Risk Assessment System Based on Fuzzy Composite Evaluation and a Backpropagation Neural Network for a Shield Tunnel Crossing under a River

Xiao Liang[1,2], **Taiyue Qi**[1,2], **Zhiyi Jin**[1,2], **Shaojie Qin**[1,2] **and Pengtao Chen**[1,2]

[1]*Key Laboratory of Transportation Tunnel Engineering, Ministry of Education, Chengdu, China*
[2]*School of Civil Engineering, Southwest Jiaotong University, Chengdu, China*

Correspondence should be addressed to Taiyue Qi; qitaiyue85@126.com

Received 17 September 2020; Revised 21 October 2020; Accepted 26 October 2020; Published 17 November 2020

Academic Editor: Yong Liu

Constructing a shield tunnel that crosses under a river poses considerable safety risks, and risk assessment is essential for guaranteeing the safety of tunnel construction. This paper studies a risk assessment system for a shield tunnel crossing under a river. Risk identification is performed for the shield tunnel, and the risk factors and indicators are determined. The relationship between the two is determined preliminarily by numerical simulation, the numerical simulation results are verified by field measurements, and a sample set is established based on the numerical simulation results. Fuzzy comprehensive evaluation and a backpropagation neural network are then used to evaluate and analyze the risk level. Finally, the risk assessment system is used to evaluate the risk for Line 5 of the Hangzhou Metro in China. Based on the evaluation results, adjustments to the slurry strength, grouting pressure, and soil chamber pressure are proposed, and the risk is mitigated effectively.

1. Introduction

Tunnel construction is affected by environment, technology, and management and is prone to safety accidents. For example, the world-famous Seikan Tunnel in Japan had four major flooding accidents during its 16-year construction period, with the maximum volume of water ingress being 121.000 m^3 [1]. In Norway, the Vardø Tunnel had two collapses during construction; the Ellingsøy Tunnel collapsed during construction because the working face was in a fault and fragmentation zone, and the top of the tunnel collapsed by 8–9 m; construction of the Oslofjord Tunnel was halted because of flooding problems, and the tunnel was only completed with difficulty by using the freezing method [2]. In Denmark, the Great Channel Tunnel experienced a flooding incident [3]. In China, the Dapu Road Tunnel under the Huangpu River in Shanghai had serious problems with water, flooding, and mud leaks, all of which affected tunnel safety [4]. The Xiang'an section of the Xiamen Undersea Tunnel also suffered water-surge collapse during construction, with the rate of water ingress reaching 120 m^3/h; a major safety accident was prevented by the timely adoption of measures such as blocking drainage, support reinforcement, and reinforcement by high-pressure rotary spraying [5]. The above engineering examples show the necessity of conducting risk assessments to ensure tunnel construction safety.

Sinfield and Einstein [6] noted the need for risk assessment before implementing new tunnel technologies, and they proposed the DAT (Decision Aids for Tunneling) method to simulate tunnel construction and study its effects. Social and economic risks and the optimization of economic risks are studied and applied to tunnels under construction in the Netherlands. Hong et al. [7] used event tree analysis to study the risks of tunnel construction; they considered the probability of accidents during construction with practical problems and proposed countermeasures. Beard [8] reported on the safe construction of tunnels. Much work has been done in risk assessment and decision-making, and a more rational decision-making system for tunnel safety has

been proposed. Hyun et al. [9] used fault tree analysis and hierarchical analysis to assess the level of mechanically related risks in shield tunnels. Chen and Huang [10] proposed some concepts for defining the risks in tunnels and underground works, developed risk analysis and evaluation models, and introduced the concept of risk value and risk indicators; a risk study of shield tunnels in soft soil areas was carried out, and seven major types of possible losses were proposed. Wang et al. [3] identified the primary risk factors in the construction of submarine tunnels based on the basic theory of risk management and tunnel construction, and they gave corresponding control measures for important risk factors. Ying et al. [11] conducted (i) a risk analysis of an underpass tunnel using fuzzy comprehensive evaluation and (ii) a risk assessment of Line 1 of the Hefei Metro in China in combination with the risk characteristics of the associated underpass roadbed construction environment. Zhang et al. [12] used hierarchical analysis and fuzzy decision-making to determine the likelihood of collapse risk events, determine qualitative indicators by expert judgment, establish a collapse risk evaluation system, and assess the collapse risk of the Mountain Ridge Tunnel. Zhang et al. [13] studied the tunnel risk factors of adjacent bridges to determine a tunnel risk model, and they verified it by engineering examples.

Previous studies have classified the risks of tunnel engineering, defined the concepts of risk indicators and risk factors, and proposed a corresponding risk assessment system. However, the existing risk assessment system contains many qualitative indicators, and the weights of qualitative indicators are determined mainly by expert experience, which has high uncertainty. Moreover, most previous studies assessed the collapse deformation of tunnels constructed by mining, and few studies have assessed the construction risks of shield tunnels under rivers. Therefore, considering the actual risk situation of a tunnel crossing under a river as part of Line 5 of the Hangzhou Metro in China, the present paper (i) identifies the risk, (ii) determines the risk factors and indicators, (iii) carries out quantitative research through numerical simulation, (iv) uses various mathematical methods for risk evaluation and comparison, and (v) combines with the project site data validation analysis and establishes a risk evaluation system for the tunnel crossing under the river.

2. Engineering Background

The right and left lines of Line 5 of the Hangzhou Metro between Tonghui Road Station and South Train Station are 1652.695 and 1655.575 m, respectively, in length. The tunnel is constructed by the shield and mining methods. The shield tunnel starts at South Train Station and goes down through South Train Station and its West Square, whereupon the mining method is adopted when crossing Mountain Hushan. Then, the tunnel goes in turn through the Langjia road bridge, after the North Trunk Police Station, finally reaching Tonghui Road Station.

Herein, the studied section is where the shield tunnel crosses the North Hushan River after the second start (i.e., 40–185 rings on the left line and 35–160 rings on the right line), as shown in Figure 1. The North Hushan River is an inland river, and the relevant hydrological data are given in Table 1.

Figure 1: Diagram of a section of the tunnel under river.

The buried depth of the tunnel is 17 m, and the water cover depth of the upper part is 5 m. The internal and outer diameters of the tunnel are 5500 and 6200 mm, respectively. The tunnel goes mainly through strata of gravelly silt clay and rounded gravel, which are treated as class-V perimeter rock. The initial design is synchronous excavation. The synchronous slurry is an inert slurry with an injection pressure of 0.2–0.3 MPa and no secondary injection. The soil bin pressure is 0.3–0.4 MPa. The tunnel comprises 350 mm thick prefabricated reinforced-concrete segments: the concrete strength grade of each segment is C50, the impermeability grades are P10 and P12, the longitudinal and circumferential directions of the segments are connected by bent bolts, and staggered seams are assembled.

3. Risk Identification and Numerical Model

Risk identification involves identifying the factors that cause risk in construction and evaluating the risk indicators. The specific steps are as follows: (i) determine the risk factors and risk indicators by combining the relevant research [14, 15] and on-site construction details; (ii) use a numerical model to simulate the risk factors, obtain the corresponding deformation value for each risk indicator, and verify the correctness of the numerical simulation through on-site measurements and comparison verification; (iii) use the formula to calculate the deformation values for the risk indicators to obtain the risk value; and (iv) establish a sample data set on which to perform quantitative analysis.

3.1. Risk Identification. Tunnel construction risks include environmental and technical ones [16]. The environmental factors refer mainly to the geological conditions affecting the tunnel, including the grade of the surrounding rock and depth of burial. The technical factors refer mainly to the design parameters and technical measures that affect tunnel safety. Combined with the analysis of shield-tunnel construction, the risk factors are as follows: grade of surrounding rock; burial depth; depth of water cover; excavation method; strength of synchronous grouting; strength of secondary grouting; grouting pressure; soil bin pressure.

The main risk events when the shield tunnel crosses under the river include the risk of landslide and water surge,

Table 1: Hydrological data for river.

Name	Width (m)	Depth (m)	Elevation of water level (m)	Elevation of river bottom (m)
North Hushan River	3	1910	57.15	0.32

so landslide and water surge are used as composite risk indicators. Each risk that triggers the combined risk is taken as a single risk indicator, and a corresponding two-level evaluation index system is established, as given in Table 2.

3.2. Numerical Model. Based on the actual situation of the studied interval, a numerical model was established using FLAC 3D with a total of 335.617 zone units, 167.900 shell units, 167.900 liner units, and 201 336 gridpoints. The model has five main parts: (i) ground surface, (ii) river bed, (iii) stratum 1, (iv) stratum 2, and (v) building. The size of the whole model is $X \times Y \times Z = \text{length} \times \text{width} \times \text{height} = 200\,\text{m} \times 200\,\text{m} \times 60\,\text{m}$, as shown in Figure 2. Horizontal displacement constraints are set in the X and Y directions of the model, while horizontal and vertical displacement constraints are set in the Z direction on the ground. The tunnel radius is 3.1 m, and the between-tunnel spacing is 10.8 m. The strata through which the tunnel passes are a silty clay layer containing gravel (stratum 1) and a layer of circular gravel (stratum 2).

The specific parameter values are given in Table 3. During the modeling process, the following basic assumptions were made: (1) the surrounding rocks are isotropic and continuous elastoplastic materials that obey the Mohr–Coulomb yield criterion and are simulated by zone elements. (2) The shield-tunnel segments are made of elastic material that is simulated by liner units, while the grouting-layer material is simulated by shell units. (3) Considering the fluid-solid coupling, the seepage model is isotropic.

3.2.1. Modeling of Risk Factors. Having established the model, it is necessary to simulate the impact of various risk factors. The "kill unit" was used to simulate the shield excavation, and surface forces were applied around the tunnel to simulate different grouting pressures. A thrust force was applied along the excavated face of the tunnel to simulate the soil chamber pressure. The simulation methods are detailed in Table 4.

3.2.2. Deformation of Risk Indicators. Numerical calculations were performed to obtain maps of the vault settlement, surface and riverbed settlement, and plastic-zone range, as shown in Figure 3. Regarding the vault settlement, extracting the displacement cloud map of the cross section at the corresponding location gives the settlement values, as shown in Figure 3(a). Regarding the surface and riverbed settlement, extracting the displacement cloud map for the corresponding locations on the surface gives the settlement values, as in Figure 3(b). Regarding the plastic zone, the stratigraphic-state cloud map is extracted for the corresponding location, as shown in Figure 3(a), and the plastic-zone length is obtained after measurement.

Table 2: Risk assessment indicators for tunnel crossing under a river.

Category	Construction risk level for tunnel under river
Combined risk indicators	Water surges; landslides
Single risk indicator	Plastic-zone extent; vault settlement; surface settlement; riverbed settlement
Risk factor	Level of surrounding rock; depth of tunnel; depth of water coverage; excavation method; strength of synchronized slurries; strength of secondary grouting; grouting pressure; soil bin pressure

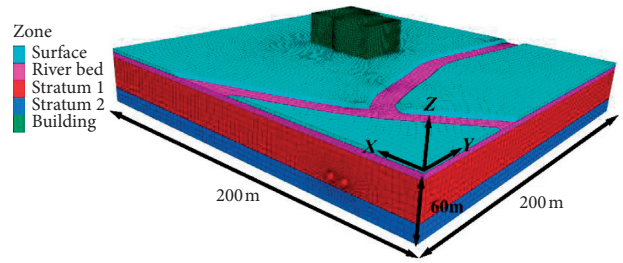

Figure 2: Schematic of numerical model.

To verify the numerical simulation results, they are compared with monitoring data and the results are given in Table 5. The simulation values for the vault and riverbed settlements differ only slightly from the measured values, the error being less than 1 mm in each case. For the surface settlement and plastic-zone range, the errors are 2.49 mm and 0.20 m, respectively. Overall, the errors are relatively small, and the data from the numerical simulation reflect the actual deformation values more accurately.

3.3. Calculation of Risk-Indicator Deformation: Risk Value. The probability of disease occurrence is determined by calculating the risk value based on the deformed value of the risk indicator. By comparing the deformation value with the normative limit [17], the risk value R_j ($j = 1 - 4$) for a single risk indicator is obtained:

$$R_j = C_j \times \frac{\text{deformation of risk indicator}}{\text{allowable value for structural deformation in codes}} \times 100\%, \quad (1)$$

Table 3: Material parameters for model.

Item	Thickness (m)	Density (kg/m^3)	Compression modulus (MPa)	Elasticity modulus (MPa)	Poisson's ratio	Cohesion (kPa)	Friction angle (°)
Surface	5	1910	4.5	—	0.35	15	11
River bed	5	1750	3.0	—	0.43	12.5	12
Stratum 1	25	2010	7.0	—	0.35	15	18
Stratum 2	15	2150	40	—	0.17	3.5	40
Segment	0.35	2500	—	34500	0.20	—	—

Table 4: Numerical simulation approach to risk factors.

Risk factor(s)	Simulation method
Level of the surrounding rock	Adjust physical parameters of soil
Depth of tunnel; depth of water coverage	Adjust overburden thickness and water pressure above the tunnel
Excavation method	Adjust excavation sequence and pacing
Strength of synchronized slurries	Adjust physical parameters of shell units
Strength of secondary grouting	Adjust physical parameters of line units
Grouting pressure	Apply surface forces along the tunnel perimeter
Soil bin pressure	Apply thrust force on excavation face

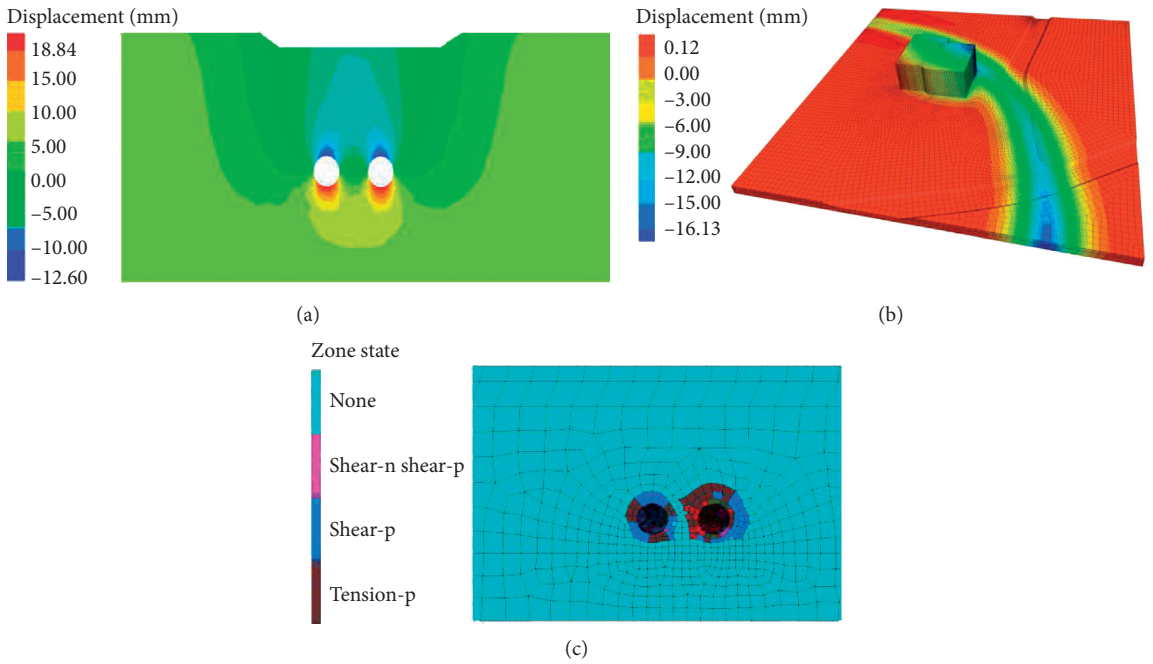

Figure 3: Cloud maps from numerical simulation. (a) Settlement of vaults. (b) Sedimentation of ground surface and river bed. (c) Range of plastic zone.

Table 5: Comparison of numerical simulation results with monitoring data.

Item	Measured value	Simulated value	Error
Settlement of vault (mm)	11.89	12.60	−0.71
Surface settlement (mm)	13.22	10.73	2.49
Settlement of riverbed (mm)	14.24	13.73	0.51
Extent of plastic zone (m)	2.30	2.50	−0.20

where C_j is the adjustment factor corresponding to each single risk indicator and takes the value of 1 using site monitoring data. The collapse risk R_A is then calculated from the single risk indicator as

$$R_A = K_a \times R_{\max} \times 100\%, \tag{2}$$

where K_a is the collapse coefficient and $R_{\max} = \max(R_j)$. Accordingly, the surge risk R_B is derived from the on-site surge risk R_{b1} and water-pressure risk R_{b2}:

$$\begin{aligned} R_{b1} &= K_{b1} \times \frac{\text{water surge}}{\text{maximum allowable water surge in design documents}} \times 100\%, \\ R_{b2} &= K_{b2} \times \frac{\text{water pressure}}{\text{maximum allowable water surge in design documents}} \times 100\%, \\ R_B &= \max(R_{b1}, R_{b2}), \end{aligned} \tag{3}$$

where K_{b1} is the surge coefficient and K_{b2} is the water pressure coefficient, generally taken as 1.

3.4. Creation of Sample Data Set. The unit scale of each risk factor is different, and the range of value distribution varies greatly, so it is impossible to calculate the value directly. Therefore, for quantitative analysis, we quantify and normalize the risk factors and indicators as given in Table 6. Quantification involves expressing some nonspecific and ambiguous factors with specific data to achieve analysis and comparison; normalization involves nonquantitative processing so that the absolute value of each factor in the system becomes some relative value relationship.

A sample set was created based on the quantitative table to provide data support for risk evaluation. Twenty-five different combinations of risk factors were designed to simulate different tunnel construction conditions, and the deformation values of the risk indicators under the corresponding conditions were obtained through numerical calculations (see Table 7).

4. Risk Assessment

During the risk evaluation process, the indicator weights are calculated by fuzzy integrated assessment and a back-propagation neural network (BPNN) to determine the correspondence between risk-indicator deformation values and risk factors.

4.1. Fuzzy Composite Evaluation. Fuzzy integrated regression models combine regression methods with fuzzy mathematics to accommodate both the fuzzy nature of the model parameters and the quantitative analytical assessment. The fuzzy regression model is determined by the relationship between risk factors and indicators [14, 15]. The data of the sample set is used to plot the relationship curves between risk factors and indicator deformation values, as shown in Figure 4, from which the following can be seen: (1) the influence curve of surrounding rock level can be approximated using a quadratic function, while those of the other factors can be approximated as straight lines. (2) The main technical factors affecting the tunnel and surface settlements are the slurry strength, grouting pressure, and soil bin pressure. (3) Improving slurry strength is effective for controlling the tunnel and riverbed settlements, and grouting pressure and soil bin pressure are the main technical factors affecting the tunnel and surface settlements. (4) The soil bin pressure is better for controlling the surface settlement.

According to the curve form of the factor-indicator deformation values in Figure 4, the fuzzy regression model corresponding to each risk indicator is established as

$$Y_i = A_1 X_1^2 + A_2 X_2 + A_3 X_3 + \ldots + A_8 X_8 + B_0, \tag{4}$$

where Y_i ($i = 1-4$) is the deformation value of the risk indicator, A_1–A_8 are the fuzzy coefficients corresponding to the risk factors, and B_0 is a constant.

Solving the fuzzy coefficients in the above equation is equivalent to solving a linear planning problem under certain constraints (see equation (5)). After solving the problem, the risk-indicator-risk-factor relationship is obtained as follows:

$$\begin{aligned} &\min = \sum_{1}^{25} \left(w_0 + w_1 X_{i1}^2 + w_2 |X_{i2}| + w_3 |X_{i3}| + \cdots + w_8 |X_{i8}| \right), \\ &Y_1 \le \left(c_0 + c_1 X_{i1}^2 + c_2 X_{i2} + c_3 X_{i3} + \cdots c_8 X_{i8} \right) + (1-h) \left(w_0 + w_1 X_{i1}^2 + w_2 |X_{i2}| + w_3 |X_{i3}| + \cdots + w_8 |X_{i8}| \right), \end{aligned} \tag{5}$$

Table 6: Quantification of risk factors.

Quantified value	x_1	x_2 (m)	x_3 (m)	x_4 (m)	x_5 (MPa)	x_6 (MPa)	x_7 (MPa)	x_8 (MPa)
0.2	VI	20	5	0	0	0	0.2	0.2
0.6	V	30	10	10	2	5	0.4	0.4
0.8	IV	40	20	20	4	10	0.6	0.6
1.0	III	50	30	30	6	15	0.8	0.8

Note. x_1–x_8 are the grade of surrounding rock, depth of burial, depth of cover, excavation interval, synchronous slurry strength, secondary slurry strength, grouting pressure, and soil bin pressure, respectively.

Table 7: Evaluation sample set.

Working conditions	X_1	X_2	X_3	X_4	X_5	X_6	X_7	X_8	Y_1 (mm)	Y_2 (mm)	Y_3 (mm)	Y_4 (m)
1	0.6	0.4	0.2	0.2	0	0	0.2	0.2	32.5	17.4	28.2	3.0
2	0.6	0.4	0.2	0.8	1	0.2	0.2	0.2	16.1	10.9	14.1	0
3	0.6	0.4	0.2	0.8	1	0.6	0.6	0.6	12.6	10.7	13.7	0
⋮	⋮	⋮	⋮	⋮	⋮	⋮	⋮	⋮	⋮	⋮	⋮	⋮
25	0.4	0.4	0.4	0.2	0	0	0.2	0.2	70.9	45.9	60.6	6.0

Notes. X_1–X_8 are the quantified values of x_1–x_8, respectively; Y_1–Y_4 are the deformation values of vault settlement, surface settlement, riverbed settlement, and plastic-zone range, respectively.

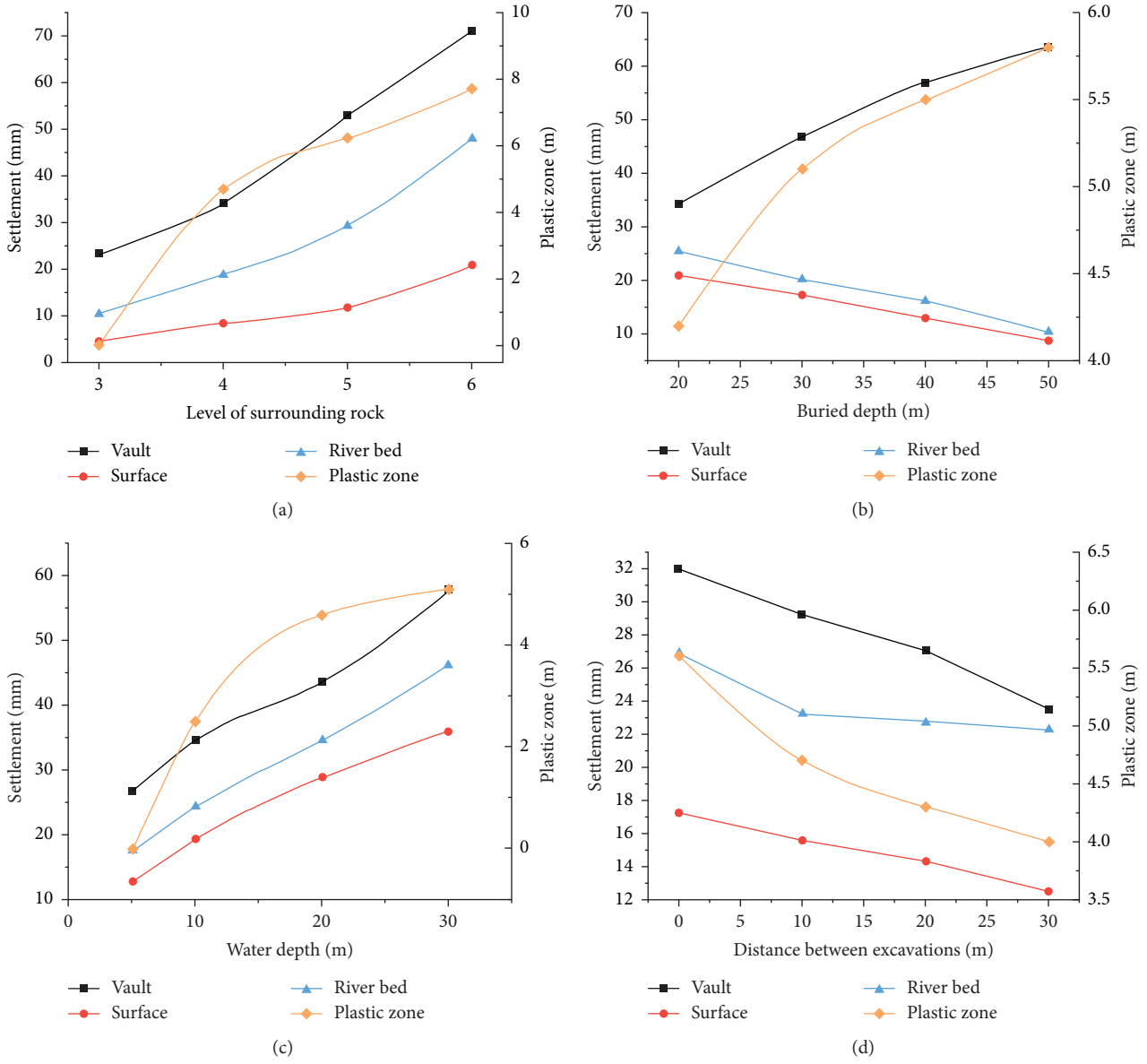

Figure 4: Continued.

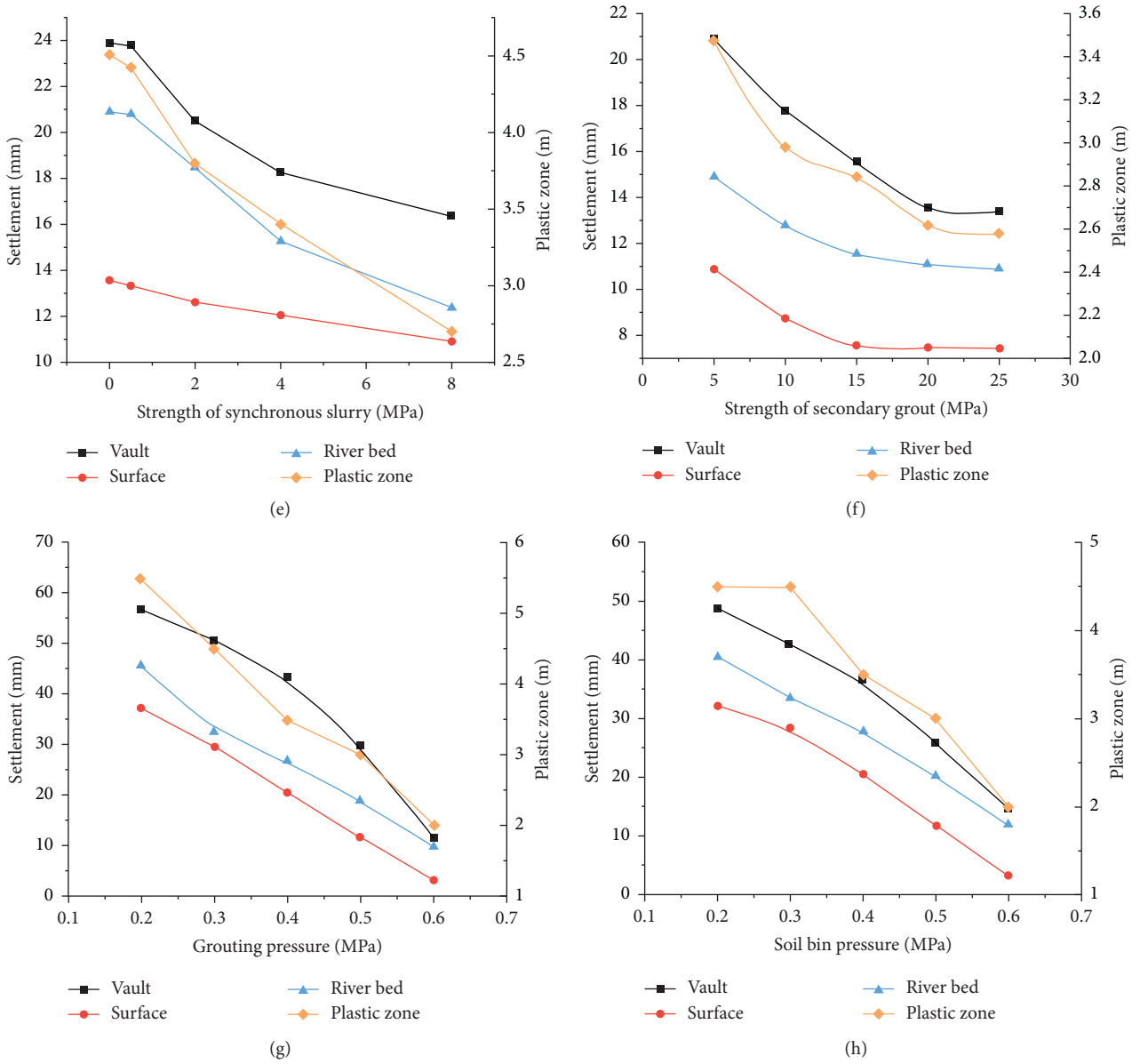

Figure 4: Risk-factor-indicator deformation value relationship diagram. (a) Perimeter rock grade. (b) Burial depth. (c) Depth of cover. (d) Excavation interval. (e) Synchronous slurry strength. (f) Secondary slurry strength. (g) Injection pressure. (h) Soil bin pressure.

$$Y_1 \geq \left(c_0 + c_1 X_{i1}^2 + c_2 X_{i2} + c_3 X_{i3} + \ldots c_8 X_{i8}\right) - (1-h)\left(w_0 + w_1 X_{i1}^2 + w_2 |X_{i2}| + w_3 |X_{i3}| + \ldots + w_8 |X_{i8}|\right), \quad (6)$$

$$Y_1 = 63.09 - 46.15X_1^2 + 13.07X_2 + 18.21X_3 - 4.15X_4 - 23.17X_5 + 4.19X_6 - 28.36X_7 - 17.61X_8,$$

$$Y_2 = 49.64 - 24.64X_1^2 - 24.58X_2 + 22.06X_3 - 5.97X_4 - 7.10X_5 + 3.14X_6 - 16.72X_7 - 11.13X_8, \quad (7)$$

$$Y_3 = 47.66 - 35.64X_1^2 - 27.43X_2 + 31.19X_3 - 9.89X_4 - 13.29X_5 + 6.36X_6 - 21.49X_7 - 12.37X_8, \quad (8)$$

$$Y_4 = 7.59 - 4.63X_1^2 - 0.16X_2 + 1.69X_3 - 1.59X_4 - 2.99X_5 + 1.53X_6 - 3.15X_7 - 2.11X_8. \quad (9)$$

Based on equations (6)–(9), the deformation values of each risk indicator can be calculated. To judge the fitting between the initial calculated values and the actual values of the sample (i.e., the target values), we draw scatter plots as shown in Figure 5. These show that almost all of the differences between the calculated and target values of the vault

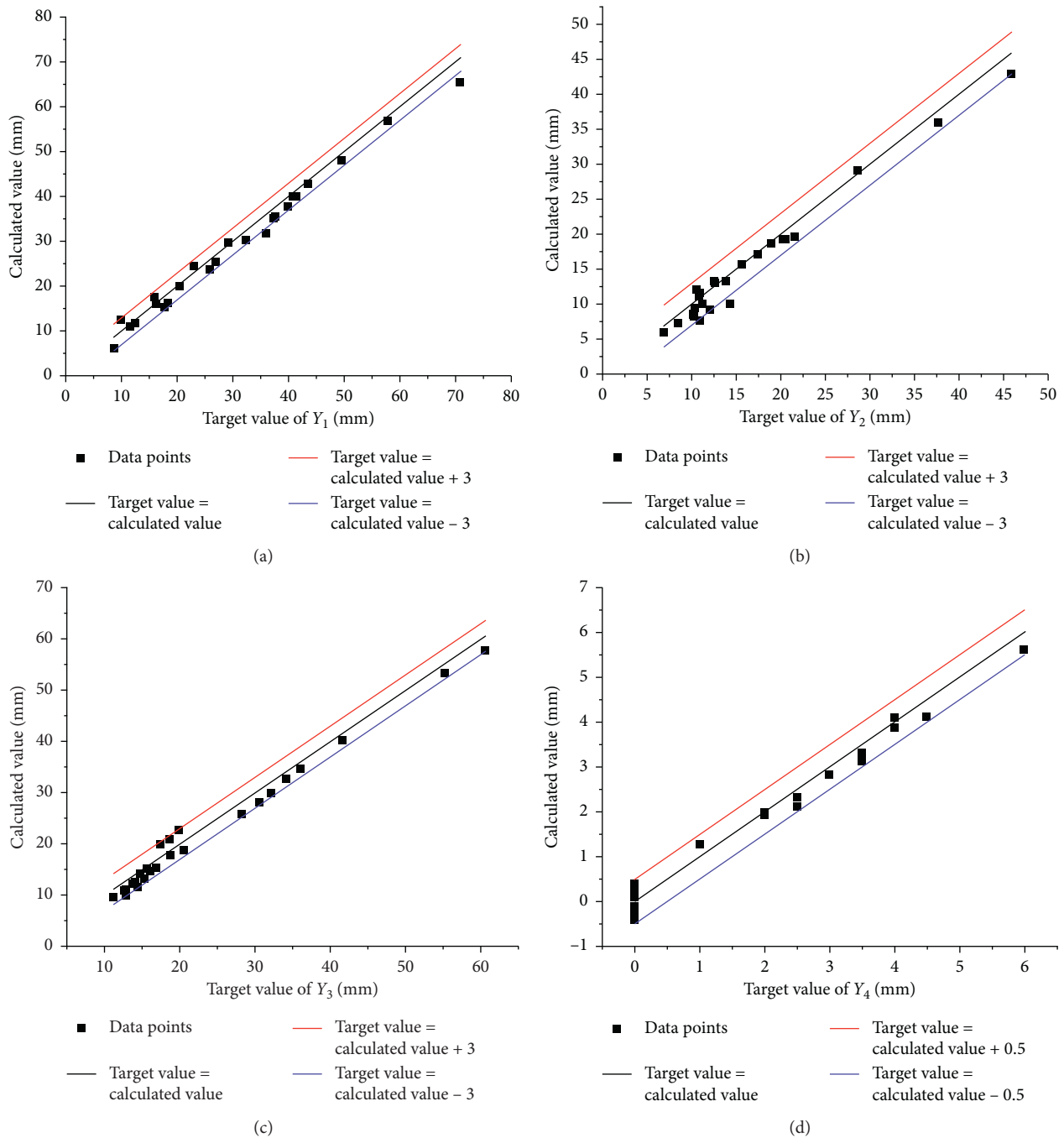

FIGURE 5: Diagrams of relationships between calculated and target values. Deformation values of (a) vault settlement, (b) surface settlement, (c) riverbed settlement, and (d) plastic-zone range.

settlement are within 3 mm, with only one error of more than 3 mm; the values are close to and slightly smaller than the target values. Almost all the calculated values of the surface settlement deformation are the same as the target values; only two errors are more than 3 mm. Although there are two errors greater than 3mm, the accuracy can still meet the required accuracy of the engineering. The fitting for the riverbed-settlement deformation is good, with all errors controlled to within 3 mm: the calculated values are slightly smaller than the target values, but the accuracy meets the basic requirements; however, when the deformation value is larger, so is the calculation error.

4.2. Risk Evaluation by Backpropagation Neural Network. A BPNN learns on a set of samples containing input and output values, reflecting the mapping relationships in the samples. The learning process comprises forward and

backward propagation. The forward propagation passes the input values from the samples to the implicit layer for processing according to a specific training method and then passes them to the output layer to obtain the output values and calculate the errors with respect to the actual values. The backward propagation then corrects the weights according to the errors and learns iteratively to reduce the global error of the network [18].

To establish the corresponding BPNN for the present case, the risk-factor quantification values X_1–X_8 are selected as the input values and the risk-indicator deformation values $Y_1 - Y_4$ are selected as the output values. It contains one implicit layer and one output layer. The Bayesian regularization algorithm is selected as the training method to correct the data of the implicit and output layers by adjusting the weights and intercepts. The network structure is shown in Figure 6.

Among the 25 data sets, 21 were used to train the BPNN on the samples, and the remaining four were used for testing to evaluate the learning effect. After the learning test of the sample sets corresponding to the four evaluation indicators through MATLAB 2016a, the results are shown in Figure 7, where R is the coefficient of determination; the range of R is [0, 1], and the closer to 1, the better the fitting effect of the model. It can be seen that the training set has a good training effect and a high degree of fit. The learning effect of vault settlement is the best (degree of fit = 1), and that of plastic-zone range is the worst (degree of fit = 0.95), which overall meets the requirements; the prediction effect of the test set of each indicator is basically the same, all at 0.98. On the whole, the learning and prediction performance of the BPNN meets the requirements of risk evaluation.

4.3. Comparison. After calculating using fuzzy comprehensive evaluation and the BPNN, the results of the two methods are compared. To analyze the results more intuitively, the errors of the calculated values of the two methods and their distribution ranges are calculated statistically, and the error distribution maps are shown in Figure 8. Overall, the values calculated using fuzzy comprehensive evaluation are smaller than the target values, whereas those calculated using the BPNN are larger than the target values. Regarding the ground settlement, the values calculated using fuzzy comprehensive evaluation have two groups of errors of more than 3 mm, whereas those calculated using the BPNN have only one group of errors on more than 3 mm. Regarding riverbed settlement, the values calculated using the fuzzy evaluation method are small and those calculated using the BPNN are large, but the values calculated using each method are controlled to within 2 mm, which is the best fit. Regarding the plasticity range, the error values with fuzzy comprehensive evaluation are concentrated between −0.1 and 0.1 m (a total of 19 groups) and those with the BPNN are concentrated between −0.1 and 0.3 m (a total of 22 groups); overall, the errors are small and have a concentrated distribution, and the fit is better.

Most of the values calculated using fuzzy integrated evaluation are smaller than the target values, which may underestimate the potential risk. There are a few large numerical errors, and although there are some errors when the deformation is large, overall the errors of settlement deformation can be controlled to within 3 mm, and the distribution error of plastic area is also tiny, which meets the accuracy requirements. Most of the values calculated with the BPNN are larger than the target values, and construction design following that method may be conservative. The ranges of error distribution are more concentrated, and there are fewer cases of large errors, so the overall performance is better. If the calculated values are larger than the target values, then construction design according to this method may be conservative. In summary, both methods meet the evaluation requirements, but there are certain shortcomings. The site construction design should be determined according to the specific circumstances of the specific method.

5. Risk Response and Control Management

5.1. Criteria for Risk Levels. In the risk assessment, combined with the risk index system and concerning the tunnel monitoring measurement, design, and construction-related specifications [14], the risks of surface settlement, vault settlement, support stress, collapse, and surge are classified into four levels according to the risk index calculation results, as given in Table 8.

5.2. Calculation of Engineering Examples. The environmental and technical parameters of the Hangzhou Metro Line 5 tunnel under the river are introduced into the fuzzy comprehensive evaluation system and the BPNN evaluation system to calculate the risk value and rating and to propose countermeasures (see Table 9). It can be seen that the fuzzy comprehensive evaluation score is slightly lower than the BPNN score, but the risk level of judgment is consistent; that is, according to the original design construction, the surface settlement and vault settlement deformation is large, and the risk of landslides and water seepage is high.

The evaluation results suggest that the design parameters should be adjusted as follows:

(1) Adjust the excavation spacing during the double-line tunnel excavation. After the left-line tunnel is excavated by 30 m, the excavation of the right-line tunnel begins. Always ensure that the excavation interval of the double-line tunnel is more than 30 m to reduce the disturbance caused by the simultaneous construction of the double-line tunnel.

(2) Replace the grouting material for synchronous grouting. Synchronous grouting can fill the gaps between the tunnel and the soil, reduce the settlement amount, and enhance the waterproof performance of the tunnel. The grouting material was changed from the original inert slurry to cement active slurry, the grouting amount was controlled at 5.5 m^3/ring, the slurry consistency was 11 ± 0.5 cm, and the bulk density was 1.70 ± 0.1 g/cm^3. The initial setting time of the slurry was 6 h, the early strength

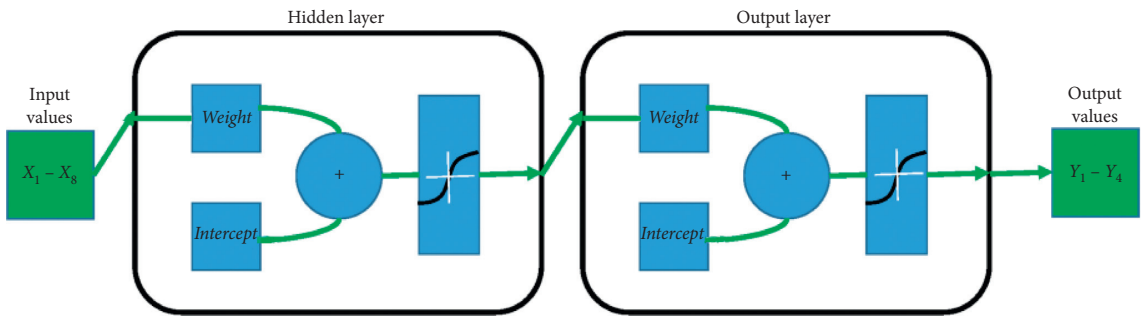

Figure 6: Structure of neural network.

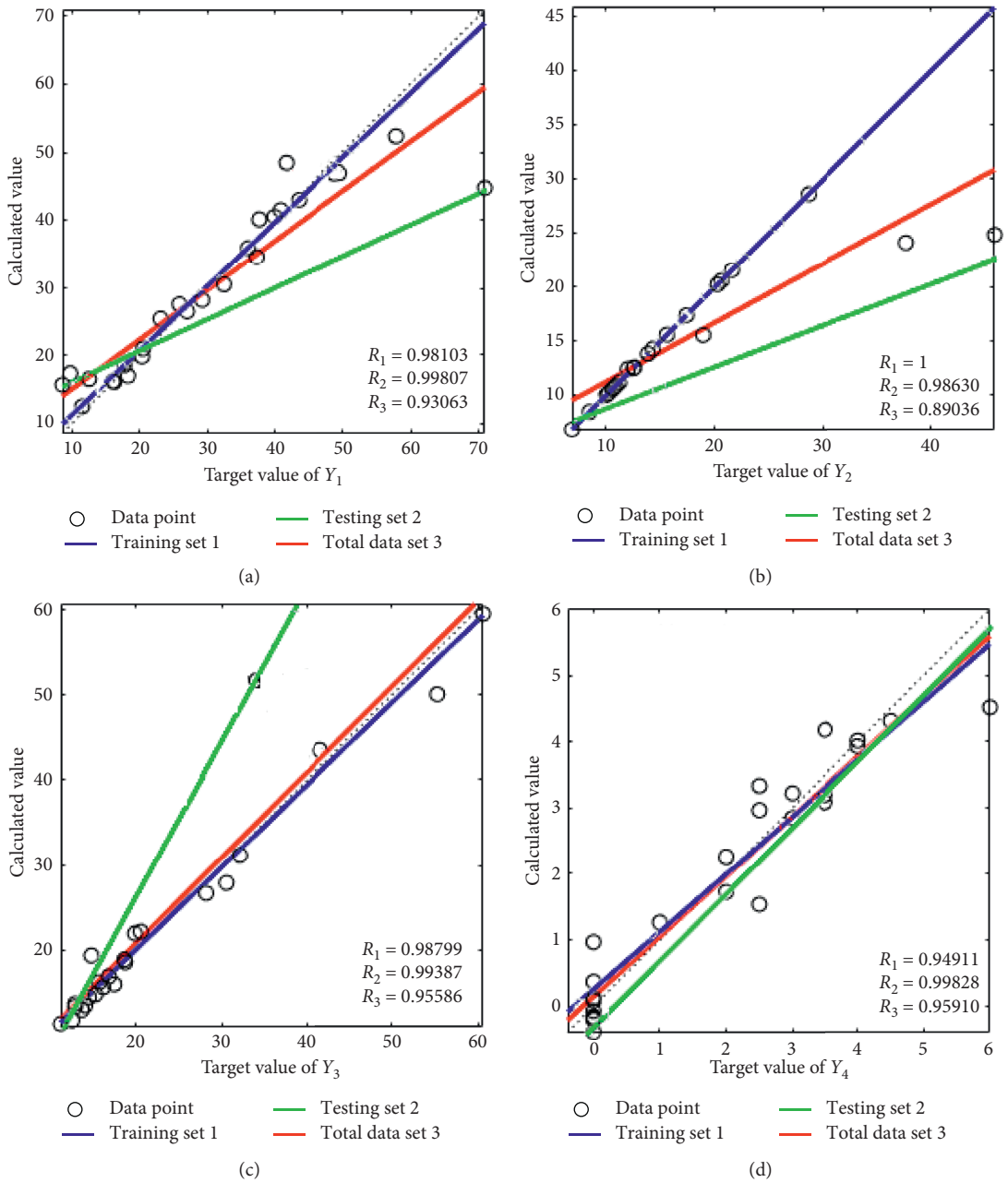

Figure 7: Diagrams of training effect: deformation values of (a) vault settlement, (b) surface settlement, (c) riverbed settlement, and (d) plastic-zone range.

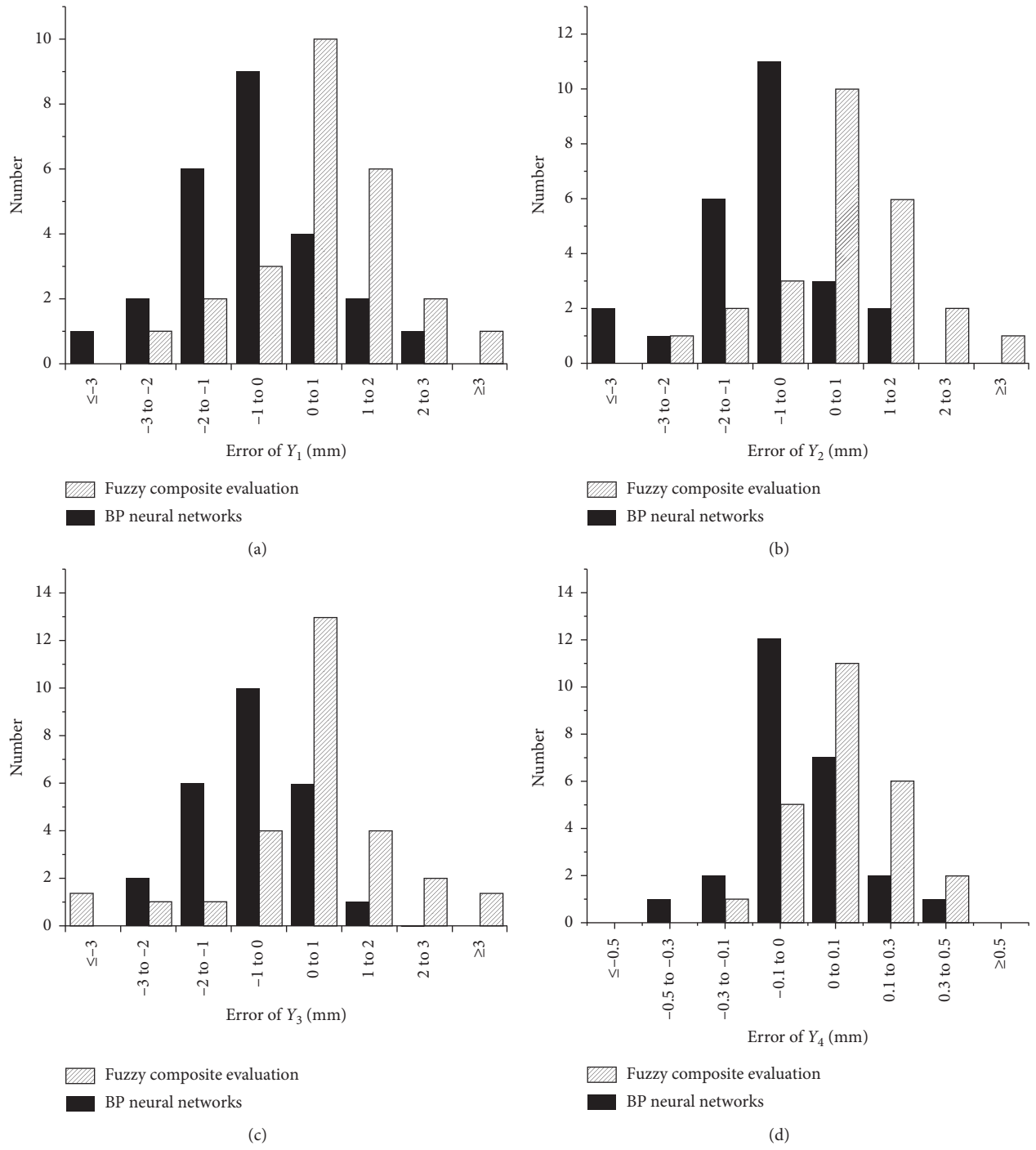

Figure 8: Diagrams of error comparison.

Table 8: Criteria for risk levels.

Risk values	0–40%	40–70%	70–85%	85% or more
Risk level	Low	Medium	High	Very high
Treatment	No risk treatment measures or monitoring required	Enhanced monitoring, but no need for risk treatment measures	Risk management measures and enhanced monitoring	Highly focused and avoidant, mitigating risk at all costs

Table 9: Assessment results.

Item	Fuzzy composite evaluation	Risk evaluation by BPNN
Single risk item	Vault settlement, ground settlement, and leakage	Vault settlement, ground settlement, and leakage
Combined risk items	Landslides and water seepage	Landslides and water seepage
Risk-indicator value	$R_A = 78\%$; $R_B = 73\%$	$R_A = 81\%$; $R_B = 73\%$
Risk level	High risk	High risk
Countermeasures	Adjust the spacing of tunnel excavation for double lines to reduce disturbance; improve the intensity level of synchronous slurry; carry out double-liquid grouting after synchronous grouting; increase grouting pressure and soil bin pressure appropriately to control sedimentation; reduce digging speed; carry out stratum reinforcement; monitor in real time and adjust grouting parameters in time	

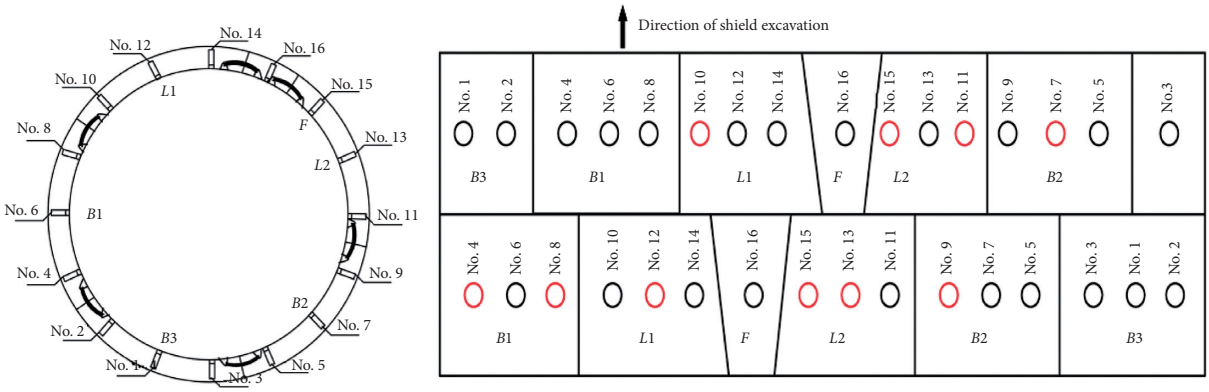

Figure 9: Schematic of reserved hole positions.

was basically reached after 24 h, and the daily compressive strength was greater than 0.3 MPa.

(3) Adjust the excavation-related parameters of the shield tunneling machine, such as the grouting pressure and soil bunker pressure. Based on the study of influencing factors in Figure 4, it is determined that the settlement can be controlled effectively by increasing the grouting pressure and soil bunker pressure. This is consistent with the conclusions obtained by relevant experts and scholars through data from numerical simulations, laboratory experiments, and field measurements. Therefore, on the basis of research and combined with engineering experience, the grouting pressure was adjusted to 0.6 MPa and the soil chamber pressure to 0.5 MPa.

(4) Conduct secondary grouting after synchronous grouting and inject double-liquid slurry for reinforcement. In the process of shield tunneling, the slurry of synchronous grouting will still have a certain gap after filling the building gap, and the existence of shrinkage deformation is also a hidden danger of ground deformation. Therefore, secondary grouting shall be carried out on the tunnel between the tail of the shield for every 10 rounds of propulsion. The construction process of the secondary grouting is as follows: (A) Select the hole position and dredge it. Reserved hole positions are selected for each ring segment, and the hole-position selection and arrangement of adjacent ring numbers are shown in Figure 9. (B) Install the long pipe for grouting. (C) Double slurry mixing. The 1 m^3 slurry consisted of 325 kg of cement and 550 kg of water, and the volume ratio of sodium silicate to cement slurry was 1 : 1. The cement strength grade was P.O. 42.5, and the water-to-cement ratio was 0.5–0.6. The initial setting time of the slurry was controlled to be 30 min, and the volume shrinkage rate was less than 5%. (D) Grouting construction: double-liquid slurry was injected at the positions of the reserved holes in the tunnel segments. The grouting pressure was 0.3–0.6 MPa, and the amount of grouting for each ring was controlled at 2 m^3. The injection was carried out sequentially from the bottom up.

(5) Strengthen the monitoring in the construction process. In the process of grouting, it is necessary to monitor in a timely manner, paying especially close attention to the formation deformation after changing the grouting parameters and adjusting the grouting parameters in time according to the deformation.

As shown by the monitoring data in Figure 10, the settlement deformation was controlled effectively after taking the above measures. As shown in Figure 11, there was no water leakage in the tunnel segments during excavation.

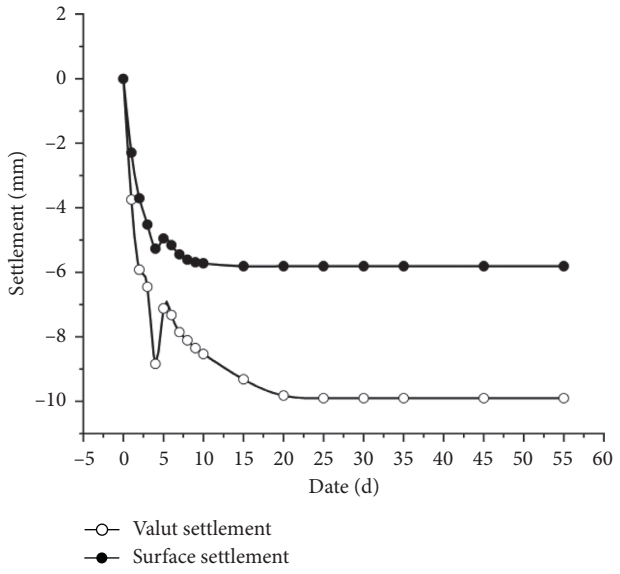

Figure 10: Settlement curves.

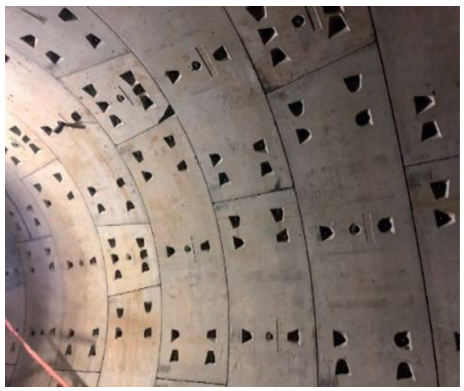

Figure 11: Site conditions of shield tunnel.

6. Conclusions

Based on the actual situation of a shield-tunnel project constructed to cross under a river, the risk factors and indicators affecting construction safety were determined, and a risk evaluation system was established. The relationship between risk factors and risk indexes was determined by numerical simulation results, showing that improving slurry strength, grouting pressure, and soil bin pressure can control settlement deformation effectively.

Fuzzy regression theory and an artificial neural network were used to analyze the sample set, establish an evaluation model, and calculate the risk values. The results showed that the risk values with the fuzzy comprehensive assessment were slightly smaller than those with the neural network assessment, but the risk levels were the same. The risk-level criteria and corresponding countermeasures were proposed, forming a complete risk evaluation system for the shield tunnel under the river.

Based on the risk assessment research, the corresponding risk-level criteria were proposed. After the risk assessment of the research area, it was concluded that when the construction is to be carried out in accordance with the original scheme, the risk level in the area would be high, and there may be collapse and seepage. Therefore, measures should be taken to mitigate the risk. Specific measures were proposed to do so effectively, such as (i) adjusting the excavation spacing, grouting pressure, and soil bunker pressure; (ii) improving the grouting materials; and (iii) carrying out secondary grouting.

However, the present study has certain deficiencies: the resolution of the numerical model is not fine enough, the selection of risk factors can be refined, and the treatment measures such as grouting materials should be optimized through experiments. All these steps should be implemented in any future work on this topic.

Data Availability

The data used to support the findings of this study are available from the corresponding author upon request.

Conflicts of Interest

The authors declare that they have no conflicts of interest.

References

[1] S. Matsuo, "An overview of the Seikan tunnel project," *Tunnelling and Underground Space Technology*, vol. 1, pp. 323–331, 1986.

[2] O. T. Blindheim, E. Grov, and B. Nilsen, "Nordic sub sea tunnel projects," *Tunnelling and Underground Space Technology Incorporating Trenchless Technology Research*, vol. 20, no. 6, pp. 570–580, 2014.

[3] Y. Wang, H. Huang, and S. Li, "Risk identification and handling during construction of subsea tunnel," *Chinese Journal of Underground Space and Engineering*, vol. 3, no. 7, pp. 1261–1264, 2007.

[4] Y. Liu, D. Zhang, and H. Huang, "Influence of long-term partial drainageof shield tunnel on tunnel deformation and surface settlement," *Rock and Soil Mechanics*, vol. 34, pp. 290–299, 2013.

[5] J. Tong, "Construction for water burst and collapse treatment in sand soil heading of Xiamen subsea tunnel," *Subgrade Engineering*, vol. 4, pp. 83-84, 2010.

[6] J. V. Sinfield and H. H. Einstein, "Evaluation of tunneling technology using the "decision aids for tunneling," *Tunnelling and Underground Space Technology*, vol. 11, no. 4, pp. 491–504, 1996.

[7] E.-S. Hong, I.-M. Lee, H.-S. Shin, S.-W. Nam, and J.-S. Kong, "Quantitative risk evaluation based on event tree analysis technique: application to the design of shield TBM," *Tunnelling and Underground Space Technology*, vol. 24, no. 3, pp. 269–277, 2009.

[8] A. N. Beard, "Tunnel safety, risk assessment and decision-making," *Tunnelling and Underground Space Technology*, vol. 25, no. 1, pp. 91–94, 2010.

[9] K.-C. Hyun, S. Min, H. Choi, J. Park, and I.-M. Lee, "Risk analysis using fault-tree analysis (FTA) and analytic hierarchy process (AHP) applicable to shield TBM tunnels," *Tunnelling and Underground Space Technology*, vol. 49, pp. 121–129, 2015.

[10] L. Chen and H. Huang, "Risk loss analysis during construction of soft soil shield tunnel," *Chinese Journal of Underground Space and Engineering*, vol. 1, pp. 74–78, 2006.

[11] G. Ying, P. Wang, D. Zhu, X. Lei, and Z. Qin, "Risk assessment of subway construction based on fuzzy comprehensive evaluation model," *Chinese Journal of Underground Space and Engineering*, vol. 2, pp. 539–545, 2016.

[12] C. Zhang, S. Wu, and J. Wu, "Study on risk assessment model of collapse during construction of mountain tunnel and its application," *Journal of Safety Science and Technology*, vol. 15, no. 9, pp. 128–134, 2019.

[13] Y. Zhang, L. Zhang, and X. Wu, "Hybrid BN approach to analyzing risk in tunnel-induced bridge damage," *Journal of Performance of Constructed Facilities*, vol. 33, no. 5, Article ID 04019048, 2019.

[14] J. Jia, B. Yan, C. Xiao, Y. Lai, and Y. Guo, "Risk analysis and assessment of shield tunnel construction under-crossing the Yellow River," *Chinese Journal of Underground Space and Engineering*, vol. 15, no. 5, pp. 1582–1590, 2019.

[15] D. Lin, M. Lei, H. Cao, and Y. Li, "Study on construction risk of shield tunnel under-passing existing railway by fuzzy comprehensive evaluation," *Journal of Railway Science and Engineering*, vol. 15, no. 5, pp. 1347–1355, 2018.

[16] Ministry of Railways, *Interim Provisions on Risk Assessment and Management of Railway Tunnels*, China Railway Publishing House, Beijing, China, 2008.

[17] X. Dai, B. Zhang, and Z. Yan, "Application of finite cloud model and distance discrimination in slope stability evaluation," *Journal of Railway Science and Engineering*, vol. 15, no. 1, pp. 71–78, 2018.

[18] X. Liang, T. Qi, T. Qi, Z. Jin, and W. Qian, "Hybrid support vector machine optimization model for inversion of tunnel transient electromagnetic method," *Mathematical Biosciences and Engineering*, vol. 17, no. 4, pp. 3998–4017, 2020.